arXiv:1410.4205v1 [cond-mat.supr-con] 15 Oct 2014

Proximity-induced superconductivity and Josephson critical current in quantum spin Hall systems

Hoi-Yin Hui, Alejandro M. Lobos, Jay D. Sau, and S. Das Sarma
Condensed Matter Theory Center and Joint Quantum Institute, Department of Physics, University of Maryland, College Park, Maryland 20742-4111, USA.

(Dated: October 17, 2014)

We consider recent experiments on wide superconductor-quantum spin Hall insulator (QSHI)-superconductor Josephson junctions, which have shown preliminary evidence of proximity-induced superconductivity at the edge-modes of the QSHI system based on an approximate analysis of the observed Fraunhofer spectra of the Josephson critical current as a function of the applied magnetic field. Using a completely independent exact numerical method involving a non-linear constrained numerical optimization, we calculate the supercurrent profiles, comparing our results quantitatively with the experimental Fraunhofer patterns in both HgCdTe and InAs-GaSb based QSHI Josephson junctions. Our results show good qualitative agreement with the experiments, verifying that the current distribution in the 2D sample indeed has peaks at the sample edges when the system is in the QSHI phase, thus supporting the interpretation that superconductivity has indeed been induced in the QSHI edge-modes. On the other hand, our numerical work clearly demonstrates that it will be very difficult, if not impossible, to obtain detailed quantitative information about the super-current distribution just from the analysis of the Josephson Fraunhofer spectra, and, therefore, conclusions regarding the precise width of the edge modes or their topological nature are most likely premature at this stage.

PACS numbers:

I. INTRODUCTION

Topological superconductors (TSC) are a special class of materials characterized by the presence of a superconducting gap in the bulk, and topologically protected gaples Majorana-fermion modes at the edges.[1] In particular, Majorana zero-energy modes (MZMs) are predicted to emerge as localized domain-wall-type excitations at the boundaries of a one-dimensional (1D) TSC wire[2], or at the vortex cores of a two-dimensional (2D) TSC system[3,4]. MZMs have become the focus of an intense research activity due to their non-Abelian braiding statistics, a property that could pave the way to implement decoherence-free topological quantum computation platforms.[2,5–7] While intrinsic TSC materials (with the appropriate topological order parameters occurring naturally in the system) are scarce in nature, in recent years this field has become increasingly active due to a number of theoretical proposals predicting topological superconductivity in hybrid structures such as the interface of topological insulator (TI)/SC[8,9] or semiconductor/SC[10–13] heterostructures. In these hybrid systems, an effective topological superconductivity and MZMs arise from specific band structure engineering which combines spin-orbit coupling, spin splitting, and proximity effect induced by ordinary s-wave superconductors to produce the appropriate topological order parameter. Experiments implementing some of these proposals have reported preliminary evidence of MZMs in hybrid structures, generating a great deal of interest in the community.[14–19]

In a seminal work[8], Fu and Kane proposed to realize a TSC at the interface between a standard s-wave SC and a TI. In the case of a quantum spin Hall insulator (QSHI), i.e., a 2D time-reversal invariant TI with 1D helical edge modes, a 1D TSC with localized MZMs is predicted to emerge at the interface with a proximate bulk SC (if in addition the time reversal invariance is also broken somehow – a necessary condition for the existence of localized MZMs). Experimental progress along this direction has been achieved recently in HgTe/HgCdTe quantum wells[20] and in InAs/GaSb quantum wells[21], two systems which have been predicted to enter the QSHI regime by tuning the chemical potential in the band minigap or controlling the well thickness. In the absence of a proximate SC, these 2D systems exhibit signatures of edge-current transport in both electrical measurements[22,23] and scanning SQUID microscopy experiments[24,25]. In particular for InAs/GaSb quantum wells contacted with superconducting indium (In) leads, Knez *et al*[26] demonstrated perfect Andreev reflection at the interface, as expected for time-reversal protected QSH edge-modes where backscattering is inhibited. This already indicates the exciting possibility of achieving topological superconductivity in QSHI systems.

However, the above experiments do not conclusively show the presence of supercurrents flowing only at the edges of the sample, as required in the Fu-Kane scenario for the existence of topological superconductivity and Majorana modes. Motivated by this question two experimental groups[20,21] recently performed measurements of the critical current $I_c(\Phi)$ flowing across SC-QSHI-SC Josephson junctions threaded by a magnetic flux $\Phi = B.S$ (with S the effective area of the junction and B an externally applied magnetic field perpendicular to the junction area). The resulting Josephson critical current variation as a function of the applied

magnetic field, often referred to as the Fraunhofer interference pattern $I_c(\Phi)$ vs Φ in the superconducting electronics literature, can in principle be deconvoluted to extract the current density profile $J(x)$ flowing across the width W of the junction, following a procedure suggested by Dynes and Fulton[27] a long time ago. The experiments, as analyzed using the Dynes-Fulton procedure, clearly show the presence of supercurrent localized at the edges of the sample precisely when the chemical potential is tuned across the (expected) QSHI regime, and a more uniformly distributed bulk supercurrent profile in the non-QSHI phase. Based on a quantitative deconvolution of the observed Fraunhofer patterns using the Dynes-Fulton procedure, superconducting edge-modes of widths 180-408 nm in the HgTe/HgCdTe system[20] and 260nm in InAs/GaSb system[21] were reported. These experimental results, putatively showing the presence of superconducting edge modes in the QSHI phase, are *indirectly* consistent with the presence of 1D TSC predicted by the Fu-Kane scenario, but no definitive evidence for either the Majorana edge modes or topological superconductivity has emerged yet.

It should be noted that the experiments in Refs. 20,21 have made use of a certain number of highly simplifying assumptions (inherent to the Dynes-Fulton analysis) which could potentially compromise the interpretation of the experimental data, namely: 1) the Josephson supercurrent density flowing in the junction (i.e., current-phase relation) has been assumed to have a simple sinusoidal form[28], i.e.,

$$J_s(x) = J(x)\sin(\beta x + \varphi), \tag{1}$$

where $\beta \equiv 2\pi L_J B/\Phi_0$, with L_J the effective length of the junction and Φ_0 the quantum of flux, and φ an arbitrary uniform superconducting phase difference across the junction. Strictly speaking, this assumption (i.e. the sinusoidal form for the Josephson current) is only justified in the short-junction limit, when $L \ll \xi$, where L is the physical length of the junction and ξ is the coherence length in the SC contacts, and $L \ll \lambda_J$, where λ_J is the Josephson penetration depth[28,29]. Although these are reasonable assumptions in many situations, in Refs. 20,21 the parameter ξ is not really known in the QSHI-SC junctions. We do expect the Josephson penetration depth to be rather large in general ($\tilde{}$ 1mm or so), and given that any proximity-induced superconducting gap in the 2D semiconductor is likely to be small, the coherence length (going as the inverse of the induced gap) should also be large in the systems of interest. Therefore, the sinusoidal approximation of Eq. (1) for the Josephson current seems reasonable, but perhaps not absolutely compelling because of the lack of information on the microscopic parameters of the junction. Another important requirement for the validity of (1) is that the transparency of the contact must be small (i.e., transmission parameter $D \ll 1$)[29]. In the case of InAs/GaSb system the transmission at the SC/QSHI interface was estimated to be of order unity (i.e., $D \simeq 0.7$), a regime where the functional form of Eq. (1) is no longer valid.[26] 2) Furthermore, it is assumed in the analyses of Refs. 20,21 that the dimensions of the junction (W and L_J) are fixed by the geometry of the sample and are therefore constants throughout the experiment for a given 2D sample. However, a smooth dependence of the effective junction parameters (e.g. W and L_J) on other experimental variables (e.g., gate voltage, external magnetic field, etc.) cannot be excluded, resulting in *effective* $\tilde{W}$ and $\tilde{L}_J$ varying with experimental parameters (such as the magnetic field and the gate voltage) in some unknown manner. 3) Another complication not included in the simple assumption of Eq. (1) is the possibility of non-uniformity in the current distribution along the other dimension (i.e. the current flow direction or the y-direction) in the 2D plane which could arise from disorder and density inhomogeneity invariably present in the semiconductor material forming the QSH system. This is particularly germane for 2D QSH systems because of the poor 2D screening properties and the invariable presence of long-range Coulomb disorder in semiconductors due to random charged impurities in the environment. Thus, in principle, $J(x)$ could depend on two spatial variables, thus becoming $J(x,y)$, because of nonuniformity and inhomogeneity, which would make the problem extremely complex from a theoretical perspective. 4) Finally, even assuming that Eq. (1) is applicable, we note that the determination of the supercurrent profile $J(x)$ starting from the measured Fraunhofer spectra and using the Dynes-Fulton method is not unique since it is essentially equivalent to an inverse scattering problem where all phase information about the original unknown function one is interested in obtaining is lost in the observed pattern being deconvoluted. The critical current $I_c(\Phi) \equiv I_c(\beta)$ (i.e., the maximal supercurrent obtained by maximizing with respect to the phase parameter φ) can be expressed as

$$I_c(\beta) = \max_{\varphi}\left[\int dx\; J(x)\sin(\beta x+\varphi)\right] = |\mathcal{I}(\beta)|, \tag{2}$$

where

$$\mathcal{I}(\beta) \equiv \int dx\; J(x)\, e^{i\beta x}, \tag{3}$$

is the Fourier transform of $J(x)$. The lack of knowledge of the complex phase $\mathcal{I}(\beta) = |\mathcal{I}(\beta)|\, e^{i\theta(\beta)}$ means that different choices of $J(x)$ could reproduce, in principle, the same *observed* $I_c(\beta)$. The standard way to overcome this problem is to consider the even and odd parts of the current profile, $J(x) = J_{\rm e}(x) + J_{\rm o}(x)$, and to assume that $J_{\rm e}(x) \gg J_{\rm o}(x)$. In that case $\mathcal{I}(\beta) \simeq \int dx\; J_{\rm e}(x)\cos(\beta x)$ is purely real, and the information about the phase can be easily reconstructed taking the alternate lobes of the Fraunhofer pattern as positive and negative, eventually interpolating linearly through the minima. Then, the heights of the minima give a semiquantitative measure

of the odd part $J_{\rm o}(x)$.[20,21,27] This procedure allows to uniquely determine an *approximate* $J_{\rm DF}(x)$ where the subscript "DF" explicitly refers to the fact that the resultant unique form for $J(x)$ arises from an approximate Dynes-Fulton analysis assuming an almost-symmetric current distribution. However, while this DF assumption can be expected to hold in ideally symmetric cases, in general the presence of disorder and inhomogeneity break the reflection symmetry with respect to the center of the junction rendering this almost-even DF approximation unjustified. In particular, when $J(x) \neq J_{\rm e}(x)$, Zappe[30] showed explicitly that many different choices of $J(x)$ have the same $I_c(\beta)$, thus emphasizing a long time ago already that the DF prescription for obtaining the unknown Josephson current distribution from the observed Fraunhofer Josephson pattern could be suspect.

In view of the considerable importance of these recent experimental developments in the context of the possible existence of MZM-carrying topological superconductivity, it becomes crucial to critically examine the validity of the results obtained in Refs. 20,21 using the Dynes-Fulton procedure. In this article we determine the current density profile $J(x)$ using the Fraunhofer data reported in Refs. 20,21, using an exact numerical optimization method that allows us to eliminate the constraints of the Dynes-Fulton analysis. Specifically: a) we allow for a non-sinusoidal current-phase relation, allowing for non-vanishing transparencies $0 \leq D \leq 1$, b) we do not explicitly restrict the functional form of $J(x)$ to be $J(x) \simeq J_{\rm e}(x)$, thereby lifting the symmetry constraint inherent in the Dynes-Fulton analysis and finally, c) we impose a constraint in order to look for solutions that avoid unphysical currents flowing outside the sample, an undesirable by-product of the Dynes-Fulton prescription which is apparent in many of the extracted $J_{\rm DF}(x)$ in Refs. 20,21 where the calculated current flow often spills way outside the physical sample dimensions used in the analysis.

We emphasize that, although our theoretical analysis uses a direct numerical procedure to obtain the current distribution starting from the observed Fraunhofer pattern in the QSHI Josephson junctions lifting the nonessential assumptions and the limitations of the Dynes-Fulton procedure, we still make a number of essential approximations ourselves (all of them are also inherent in the Dynes-Fulton procedure and therefore in the experimental analyses carried out in Refs. 20,21). We assume that the current distribution is uniform in the y-direction so that the basic Josephson junction approximation applies and we also make the short-junction approximation. These approximations can only be relaxed in a microscopic approach involving a direct numerical solution of the applicable Bogoliubov-De Gennes (BdG) equations for the SC-QSHI, but such a detailed approach is way beyond the scope of the current work and may not in any case be suitable for extracting the current distribution from the observed Fraunhofer pattern. Our main accomplishment in the current work is an exact numerical analysis of the Fraunhofer patterns reported in Refs. 20,21 going beyond the narrow constraints of the Dynes-Fulton procedure and using a full numerical optimization scheme in going from the Franuhofer patterns to the current distributions while at the same time generalizing the theory to incorporate the finite transparency at the SC-QSHI interface neglected in the Dynes-Fulton theory.

The paper is organized as follows: in Sec. II we give details about our numerical method, Sec. III is devoted to the presentation of our main results and finally, in Sec. IV we give a summary and our main conclusions.

II. METHODS

We now assume that the junction is in the short-junction limit $L \ll \{\xi,\, \lambda_J\}$, and we consider a more general expression for the current-phase relation due to Haberkorn *et al.*, valid for an arbitrary transparency of the tunnel junction at the interface[31,32]

$$I_s(\varphi) = \frac{\pi\Delta}{2eR_N} \frac{\sin(\varphi)}{\sqrt{1 - D\sin^2(\varphi)}} \tanh\left[\frac{\Delta}{2T}\sqrt{1 - D\sin^2(\varphi)}\right], \tag{4}$$

where Δ is the superconducting gap, $R_N = \left[e^2 k_F^2 SD/\left(4\pi^2\hbar\right)\right]^{-1}$ is the resistance of a contact of area S, and T is the temperature. This formula interpolates between the standard expression $I_s(\varphi) \propto \sin(\varphi)$ for the Josephson current-phase relationship as in Eq. (1), valid in the tunnel limit $D \to 0$, and the Kulik-Omelyanchuk formula, $I_s(\varphi) \propto \sin(\varphi/2)\tanh\left[\frac{\Delta}{2T}\cos(\varphi/2)\right]$, valid at perfect transmission $D = 1$.[33] Based on Eq. (4), we now generalize Eq. (1) to

$$J_s(x) \propto J(x) \frac{\sin(\beta x + \varphi)}{\sqrt{1 - D\sin^2\left(\frac{\beta x+\varphi}{2}\right)}} \quad (\text{at } T = 0). \tag{5}$$

The starting point of our analysis is Eq. 5, and not Eq. 1 as used in Refs. 20 and 21 (and in the original Dynes-Fulton treatment[27]). Note that due to the square root in Eq. (5), the maximization procedure with respect to φ in Eq. (2) needed to find I_c, is *not equivalent* to taking the amplitude of the Fourier transform of $J(x)$, Eq. (3), and the analytical expression of I_c becomes very complicated and is neither transparent nor useful. Therefore, we need to perform the maximization over φ explicitly, redefining the critical current using Eq. (5) as

$$I_c(\beta, D) = \max_{\varphi}\left[\int_{-W/2}^{W/2} dx\, \frac{J(x,D)\sin(\beta x + \varphi)}{\sqrt{1 - D\sin^2\frac{\beta x+\varphi}{2}}}\right]. \tag{6}$$

In order to find the current density profile $J(x)$, we cast the problem in the form of a minimization procedure and define a (dimensionless) *cost functional* $C[J; D]$

$$C\left[J;D\right]=\frac{1}{2\beta_{\max}}\int_{-\beta_{\max}}^{\beta_{\max}}d\beta\,\left[\frac{I_c\left(\beta,D\right)-I_0\left(\beta\right)}{I_0\left(0\right)}\right]^2, \quad (7)$$

where $I_0(\beta)$ is the experimentally obtained Fraunhofer pattern (which we extract from the published data in Refs. 20,21). To treat the problem numerically, we have discretized the variables x, β and φ on a grid. For a given value of the transparency D, we compute $C[J;D]$ by first performing the integral over x for all values of β and φ in Eq. (6). Then for each value of β the integral is maximized over φ. Finally the integral over β in Eq. (7) is performed, and the value of $C[J;D]$ obtained. The numerical method is initialized with a random initial function $J_0(x_i)$, and a constrained non-linear optimization algorithm ("active-set" algorithm in Matlab) is used to search for the minimum value $C[J(x);D]$, within a relative tolerance $\epsilon = 10^{-6}$. Similar to the Dynes-Fulton case where the phase information cannot be reconstructed, we note that our numerical procedure also does not, as a matter of principle, uniquely determine the current profile because of the phase destruction problem. However, for the Fraunhofer patterns that we generate numerically from some assumed current patterns, our algorithm finds a current distribution (from the resultant Fraunhofer patterns) where the cost function is minimized to a very low value $C[J(x);D] \lesssim 10^{-3}$, which is negligible compared to the typical error bars in critical current measurements. Although the final current distribution does not typically precisely match the starting current distribution, this low residual error confirms the validity of our procedure for finding reasonably accurate solutions for the current density within our approximation scheme of assuming short junctions and uniform current distributions.

Throughout the current work, we have used the consistency check of numerically obtaining the current distribution from the Fraunhofer spectra and then recalculating the Fraunhofer pattern from the obtained current distribution comparing the resultant pattern with the starting pattern to ensure the accuracy and the validity of our analysis. We emphasize that although the first step of this procedure, i.e. obtaining the actual current distribution from a given Fraunhofer pattern for the maximum Josephson current as a function of the magnetic field is non-unique because of the loss of phase memory, the reverse step of recalculating the Fraunhofer pattern from the obtained current distribution (i.e. Eqs. (2) or (6) depending on whether $D = 0$ or not) is perfectly well-defined and unique. We believe that this second step, which has not been presented in the analyses of Refs. 20,21, is crucial in ensuring the integrity of the procedure leading to the calculation of the current distribution in the QSHI sample.

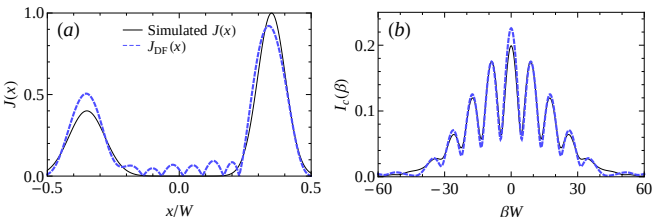

Figure 1: Consistency check of the Dynes-Fulton method. (a) Simulated $J(x)$ (continuous black line) and reconstructed $J_{\rm DF}(x)$ (dashed blue line) density profiles. (b) The corresponding Fraunhofer patterns. Although the original $J(x)$ and reconstructed $J_{\rm DF}(x)$ profiles are qualitatively similar, there is no quantitative agreement.

III. RESULTS

We first focus on the internal consistency of the Dynes-Fulton method in situations which deviate from the ideal condition $J(x) = J_{\rm e}(x)$. Given the assumptions implicit in the method, our point is that the resulting $J_{\rm DF}(x)$ is not a stable self-consistent solution upon iteration of the procedure. In other words, injecting the approximate $J_{\rm DF}(x)$, obtained with the Dynes-Fulton method, back into Eq. (3) does not allow to recover the original Fraunhofer pattern $I_c(\beta)$, from which $J_{\rm DF}(x)$ was first extracted. This is an important point (i.e., a "sanity" check to see how serious an issue the non-uniqueness aspect of the problem turns out to be) in order to test the robustness of the method. To illustrate this point, in Fig. 1(a) we show a simulated current density profile in continuous blue line, and in Fig. 1(b), the corresponding Fraunhofer pattern [obtained using Eq. (3)] is also shown as a continuous blue line. We now apply the Dynes-Fulton method, and the "reconstructed" profile $J_{\rm DF}(x)$ is shown in Fig. 1(a) (dashed black line). Note that the original $J(x)$ and reconstructed $J_{\rm DF}(x)$ profiles are *only qualitatively* similar, there is no *quantitative* agreement at all: the information about the fine details of the profile (e.g., relative heights or widths of the peaks) is not consistently reproduced. This is actually not surprising given that the initial profile $J(x)$ does not fulfill the required reflection symmetry condition $J(x) = J_{\rm e}(x)$ for Dynes-Fulton the method to be exact. Moreover, additional relevant physical mechanisms such as finite transparency (not considered in Fig. 1) can only worsen the situation. For completeness, in Fig. 1(b) we also show the Fraunhofer pattern (dashed black line) recalculated from the extracted $J_{\rm DF}(x)$. Again, the original and final Fraunhofer patterns are qualitatively very similar, but the fine quantitative details are not reproduced. We believe that this comparison between the original and reconstructed Fraunhofer patterns could serve as a useful tool to check the internal consistency of the procedure in concrete experimental situations. In the Appendix A we have performed such an internal consistency comparison using a direct digitalization of the data reported in the

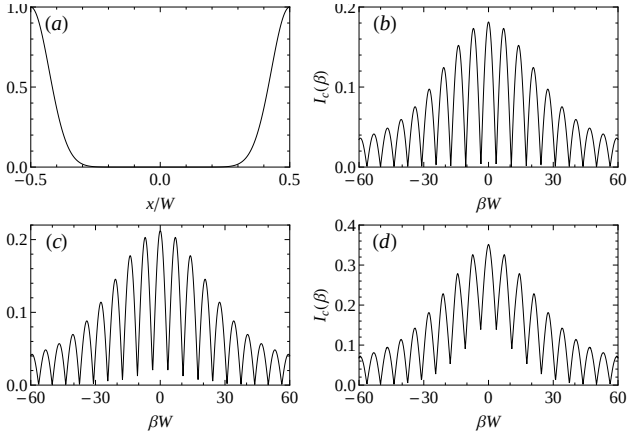

Figure 2: (a) The chosen current density. (b) the critical current against β with $D = 0$. (c) the critical current against β with $D = 0.5$. (d) the critical current against β with $D = 1$.

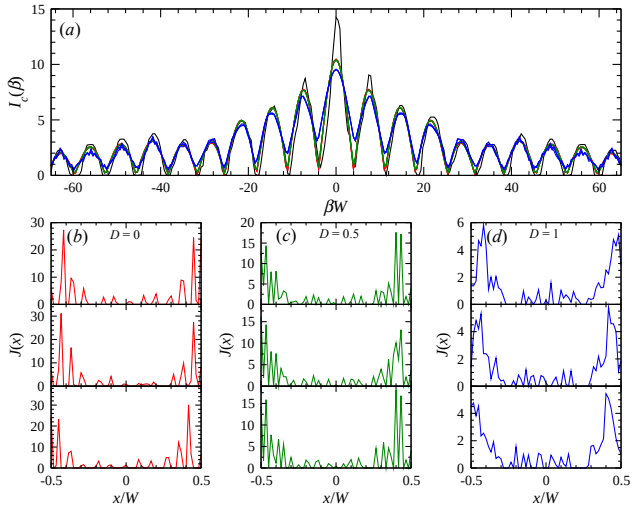

Figure 3: (a) Black line: Fraunhofer pattern obtained from digitalization of the experimental results in Fig. 2(c) of Ref. 20, where the sample is believed to be in the SQH insulating regime. Red, green and blue lines correspond to the Fraunhofer patterns obtained from the profiles below, found with our numerical minimization, for $D = 0$, $D = 0.5$ and $D = 1$, respectively. In plots (b), (c) and (d) we show the corresponding profiles for transparencies $D = 0$, $D = 0.5$ and $D = 1.0$, respectively. Slightly different profiles are obtained in each case (here we show only three for each value of D) as a consequence of the abovementioned non-uniqueness of the procedure.

QSH-SC Josephson junction experimental papers[20,21].

We now focus on the effects of a finite transparency D on the Fraunhofer patterns. As mentioned before, this is an important element of physics missing from the earlier analyses in Refs. 20,21 since the experimental QSH-SC junctions may very well be closer to the fully transparent ($D = 1$) limit than the fully non-transparent ($D = 0$) Dynes-Fulton limit. In Fig 2(a), we show an arbitrarily chosen current distribution profile $J(x)$ with the current flowing at the edges of the sample. Here we have chosen a purely even profile $J(x) = J_e(x)$ for the purpose of illustration. We next use Eq. (6) to compute the corresponding Fraunhofer pattern for transparencies $D = 0$, $D = 0.5$ and $D = 1.0$, and plot them in Figs. 2(b), 2(c), and 2(d), respectively. Note that when $D \neq 0$, these patterns exhibit a sizeable "node-lifting" effect. In the simplest Dynes-Fulton analysis (valid only for $D = 0$), the lifted nodes would have been *mistakenly* attributed to asymmetries in $J(x)$, i.e., non-vanishing odd component $J_o(x)$. We point out that this node-lifting mechanism has not been discussed previously in Refs. 20,21, and is completely different from the discussion on node-lifting in Ref. 34. With these ideas in mind, we now focus on the analysis of the experimental Fraunhofer patterns.

We first analyze the HgCdTe-CdTe data by Hart *et al.*[20] in the regime where the system is in the QSHI phase. In Fig. 3(a), the black line corresponds to the experimental Fraunhofer pattern shown in the figure 2(c) in Ref. 20. In Figs. 3(b), 3(c), and 3(d) we show the profiles resulting from our minimization procedure assuming transparencies $D = 0$, $D = 0.5$ and $D = 1.0$, respectively. Slightly different profiles are obtained for each transparency (here we show only three for each value of D) as a consequence of the abovementioned non-uniqueness of the procedure, but besides this fact, the overall features of the different plots for each value of D are consistent. Qualitatively speaking, our results agree with those of Hart *et al.* in the sense that all the numerically-obtained current density profiles *indeed exhibit distinct peaks at the edges*. Considering that our numerical search is free of predetermined assumptions inherent in the Dynes-Fulton prescription, we believe this qualitative agreement to be an important confirmation of the experimental results as definitively establishing the presence of edge super-current transport in the HgCdTe-based SC-QSHI-SC Josephson junction system. We should add for emphasis here that we have tried hard to obtain current distributions without peaks at the sample edges in the QSHI phase, but have consistently failed to find a single situation where our exact numerical procedure (with only the short junction and uniform current constraints) produces current distributions without peaks at the edges which are consistent with the experimentally observed Fraunhofer patterns in the QSHI phase reported in Ref. 20. Moreover, our reconstructed Fraunhofer patterns [shown in Fig. 3(a) as red, green and blue lines] using the numerically extracted current distributions compare fairly well with the experimental one (continuous black line). Reconstructed Fraunhofer patterns with the same color (obtained with the same value of D) fall on top of each other, and cannot be distinguished at the scale of the plots shown in Fig. 3. We take this agreement as an internal consistency check of our procedure. Finally, we note that the better agreement of the experimental Fraunhofer pattern with the

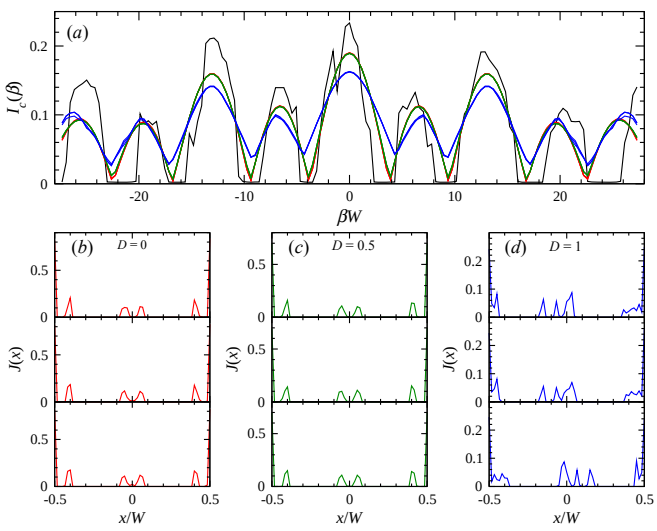

Figure 4: (a) Black line: Fraunhofer pattern obtained from direct digitalization of the experimental results in Fig. 5(a) of Ref. 21, when the sample is in the SQH insulating regime. Red, green and blue lines correspond to the Fraunhofer patterns obtained from the profiles below, found with our numerical minimization, for $D = 0$, $D = 0.5$ and $D = 1$, respectively. In plots (b), (c) and (d) we show the corresponding profiles for transparencies $D = 0$, $D = 0.5$ and $D = 1.0$, respectively. Slightly different profiles are obtained in each case (here we show only three for each value of D) as a consequence of the abovementioned non-uniqueness of the procedure.

red curve in Fig. 3(a) (i.e. $D = 0$) might be indicative of a low transparency of the contacts in the experiment of Ref. 20.

However, one should take these results with caution, in particular when considering the fine quantitative details. For instance, we note that the reconstructed Fraunhofer patterns in Fig. 3(a) do not correctly reproduce the behavior of the original experimental pattern near $\beta \approx 0$. We have checked that this is not a problem of the numerical method [e.g., failure to converge to the "true" minimum in Eq. (7)], because our code always reproduces the patterns that are numerically generated from a wide variety of current densities that are localized within the width of the wire. Therefore, the discrepancy between the experimental data and the reproduced Fraunhofer pattern suggests a break-down of (at least) one of the two main assumptions (a) the gate voltage independence of L_J or W, or (b) the short junction current-phase relation [Eq. (1) or even the more generic Eq. (5)]. Our best current guess right now is that the sample size parameters (L_J and/or W) do indeed vary with gate voltage (and magnetic field) leading to this inconsistency, but more work is needed to clarify this issue.

Our numerics also agree qualitatively (but less quantitatively compared with Ref. 20) with the results by Pribiag *et al* for the InAs-GaSb system[21]. In particular in this case, we have focused on Fig. 5(a) in Ref. 21, where the authors report an intruiguing even-odd effect in the Fraunhofer pattern when the sample is in the extreme n-doped regime (which can be thought of as the emergence of a $2\Phi_0-$periodicity in the Josephson current). The authors attribute this behavior to two possible physical mechanisms: a) a topologically-trivial mechanism corresponding to a very particular spatial current distribution containing three peaks, or b) the presence of fractional-Josephson effect, which is indeed expected when MZMs emerge at the ends of the induced TSC in the Fu-Kane scenario[8]. Both scenarios seem unlikely as mentioned already in Ref. 21. In the case of the three-peak current distribution function, a high degree of fine-tuning seems to be required to reproduce the Fraunhofer pattern. The authors of Ref. 21 argue that since the even-odd effect has been observed in at least two samples, it seems improbable that these finely tuned parameters occur in *both* samples simultaneously. On the other hand, the topological mechanism based on Josephson-coupled MZMs requires a quasiparticle poisoning time-scale which exceeds the actual experimental measurement time, an extremely unlikely scenario unless very special efforts are undertaken to suppress quasiparticle poisoning deliberately. Recently, starting from a microscopic description for transport across a SC-TI-SC junction, Tkachov *et al*[35] have predicted a temperature-driven crossover from Φ_0- to $2\Phi_0-$periodic behavior in the Fraunhofer pattern, therefore providing an alternative mechanism for this behavior. In their treatment, the authors attibute this behavior to the well-known progressive skewness of the current-phase relationship in *long junctions* as the temperature is lowered below $k_BT \ll \hbar v/\pi L$[36,37], fitting the experimental curves with parameters $L_J = 600$ nm and $\xi = 80$ nm. We point out, however, that the prescription used by Tkachov *et al* involves fixing the phase difference φ of the SCs by maximizing the supercurrent *only at zero field*, and using that value of φ for finite-B calculations of the supercurrent. Since the SC phase difference is a gauge dependent quantity, it is not clear that such a prescription obeys gauge invariance. In addition, we note that their theoretical model does not explain the observed dependence on the gate voltage, and does not allow to extract the current profile. Also, the long junction limit with very short coherence length seems inconsistent with the analyses of Refs. 20,21 as well as our own theory in the current paper. At this stage, therefore, our preference (see below) for the observed even-odd effect in Ref. 21 is that for some unknown reason the spatial current distribution does indeed have a 3-peak structure which is obviously not ruled out by any known mechanism. More future work will be necessary to clarify this issue decisively, but at this stage we believe that the short-junction approximation is perhaps not a poor approximation for the QSHI systems under consideration given the expected long coherence length and the long Josephson penetration depth applying in the problem.

Our analysis of this case is shown in Fig. 4. In Fig. 4(a), the black line corresponds to the Fraunhofer pattern obtained from direct digitalization of the experimental

results[21] in figure 5(a). Figs. 4(b), 4(c) and 4(d) correspond to different current densities $J(x)$ obtained with our numerical method assuming transparencies $D = 0$, $D = 0.5$ and $D = 1.0$, respectively. In addition, we also observe a qualitative agreement of our numerical results with the experimental Fraunhofer pattern. However, we point out here the striking apparent lack of internal consistency of the reported data, which becomes evident when comparing the experimental Fraunhofer pattern with the reconstructed one, for which we have no satisfactory explanation (see Fig. 6 in the Appendix). This inconsistency points toward a possible inapplicability of at least one of the theoretical constraints to the experimental situation applying to Ref. 21, and the possibility that the system is in the long junction limit (or perhaps there is considerable current nonuniformity) cannot be ruled out at this stage.

IV. CONCLUSIONS

We have analyzed the validity and the consistency of the Dynes-Fulton procedure[27] applied to recent Fraunhofer pattern experiments on wide SC-QSHI-SC Josephson junctions[20,21], which have shown evidence for proximity-induced superconductivity at the edge-modes of the QSHI system. Using a completely independent exact numerical method (i.e., a non-linear constrained numerical procedure, see Section II) to analyze the experimental data extracted from Refs. 20,21, we obtain the current profiles in Figs. 3 and 4 which agree qualitatively (but, not quantitatively) with the conclusions in Refs. 20,21.

Generally speaking, our results *qualitatively* reproduce current distributions with peaks at the 2D sample edges when the system is in the QSHI phase. Given that our method is completely free from the nonessential approximations of the Dynes-Fulton analysis (i.e., vanishing transparency $D = 0$ of the SC-QSHI contacts, symmetric current distributions, and profiles extending beyond the physical region $-W/2 < x < W/2$), we find that our results support the existence of proximity-induced superconductivity at the edge-modes of the QSHI. This is of course highly encouraging from the perspective of the eventual emergence of topological superconductivity with Majorana zero modes in quantum spin Hall systems.

Our work also clearly shows that the Dynes-Fulton prescription for obtaining the supercurrent spatial distribution from the observed Fraunhofer pattern has a number of intrinsic limitations, stemming from its simplicity and the various underlying approximations. For instance, we have analyzed the internal consistency of the method by comparing the original (i.e., experimental) Fraunhofer pattern with the reconstructed pattern obtained from the extracted current distribution $J_{\mathrm{DF}}(x)$ (see Figs. 5 and 6 in the Appendix). While in some cases the method seems to be reasonably successful in reproducing the original pattern, we note that in general there is a lack of quantitative agreement, which seems to be generic and inherent to the method itself stemming from the non-unique nature of the inverse scattering problem it is trying to solve. Moreover, we note that the quantitative prediction of the Fraunhofer pattern analyses in Refs. 20,21, such as the relative height or the width of the peaks, must also be taken with a great deal of caution. We note that the reported widths of the edge-modes (~ 260 nm in the case of InAs/GaSb[21] and of $\sim 180-408$ nm in the case of HgTe/HgCdTe[20]) are about one order of magnitude larger than the expected QSH edge width obtained from band structure considerations[38]. This discrepancy remains unexplained at the moment, and cannot be addressed within the present analysis. Among the possible physical mechanisms which could account for wider edge modes, we mention strong band-bending effects at the edge (which may induce multichannel transport) and disorder/puddle effects (which make the edge modes go around the puddles, effectively enhancing the width). At this stage, the theory is not capable of providing a quantitatively accurate prediction for the size of the super-current distribution at the QSHI edges in the presence of band-bending, disorder, and proximity effect. One critically disturbing aspect of the very wide effective edge size (an order of magnitude larger than the theoretically predicted value for the topological helical edge mode which should be of the order of the QSHI "coherence length" defined by v/E_g, where v and E_g are the edge velocity and the bulk gap respectively), deduced from the Fraunhofer experiments of Refs. 20 and 21, is that the simple and widely used model of a protected helical "topological" edge mode obviously would not apply to the real samples implying (among many things) that the whole issue of inducing topological edge mode superconductivity with the associated localized Majorana zero end modes needs to be carefully thought through[39] taking into account the theoretically-unexplained very large widths of these edge modes for both HgTe-HgCdTe and InAs-GaSb QSHI systems. More quantitatively accurate experiments determining the QSHI edge electronic structure would be highly desirable in this context because it is unclear at this stage how accurate the estimated edge widths based on Fraunhofer measurements really are because of the many approximations in the theory as well as the non-uniqueness of the theory extracting a spatial supercurrent distribution from the measured Fraunhofer pattern as discussed in details in our work. It should perhaps be mentioned here as a cautionary note that for the corresponding quantum Hall (QH) edge modes, there has not been any unifying picture connecting theory and experiment for the electronic structure of the QH edges in spite of 25 years of intense activity (see, for example, H. Choi *et al*[40] and references therein).

To summarize: Our theoretical conclusion is more or less consistent with those in Refs. 20,21 showing definitive evidence for the existence of super-current edge modes in the QSHI phase of HgCdTe-CdTe and InAs-GaSb quantum well systems in spite of considerable non-uniqueness

associated with the extraction of the current distribution pattern from the observed Fraunhofer pattern. In addition, we have explicitly pointed out the inadequacy and inconsistency of the simplistic Dynes-Fulton procedure for analyzing the Fraunhofer spectra in wide Josephson junctions.

Acknowledgments

The authors acknowledge support from Microsoft Q, NSF-JQI-PFC, and NSA-LPS-CMTC. J. D. Sau acknowledges Anton Akhmerov for valuable discussions.

Appendix A: Consistency check of the experimentally reported data

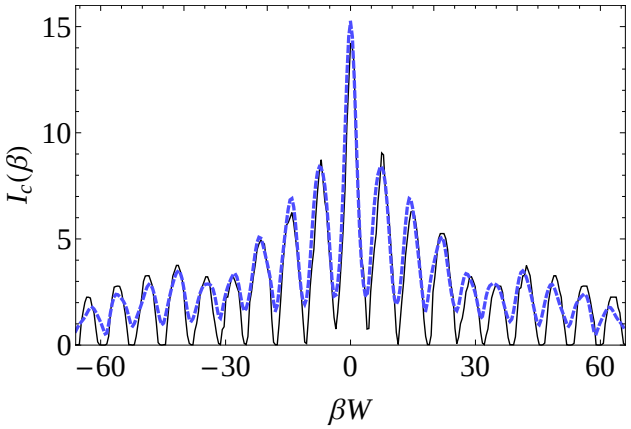

Figure 5: Fraunhofer pattern obtained from digitalization of the experimental results in Fig. 2(c) of Ref. 20 (shown as a black line), where the sample is believed to be in the SQH insulating regime. The blue dashed line corresponds to the reconstructed Fraunhofer pattern obtained from the reported current profile $J_{\rm DF}(x)$ in figure 2.d in that reference.

In this section we present an analysis of the internal consistency of the Dynes-Fulton method by comparing the original (i.e., experimental) Fraunhofer pattern (obtained from a direct digitalization of the reported experimental data) with the reconstructed pattern obtained from the reported current profile $J_{\rm DF}(x)$ (see Figs. 5 and 6). In Fig. 5 we present the data corresponding to figure 2.c in Ref. 20 as a continuous black line, whereas the dots correspond to the reconstructed Fraunhofer pattern obtained from the reported current profile $J_{\rm DF}(x)$ in figure 2.d in that reference, and Eq. 3.

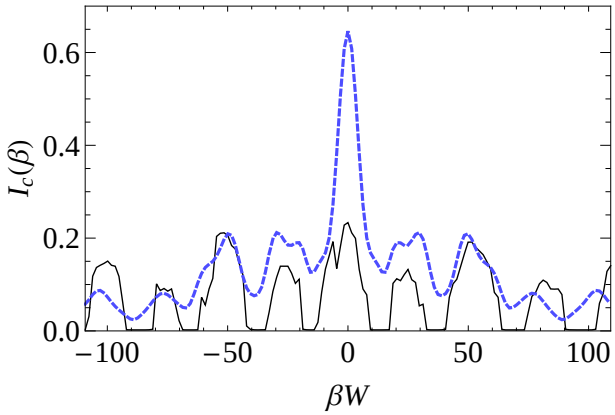

Figure 6: Fraunhofer pattern obtained from digitalization of the experimental results in figure 5(a) of Ref. 21 (shown as a black line), where the sample is believed to be in the SQH insulating regime. The blue dashed line corresponds to the reconstructed Fraunhofer pattern obtained from the reported current profile $J_{\rm DF}(x)$ in figure 5.b in that reference.

The corresponding analysis for the data reported by Pribiag *et al*[21] is shown in Fig. 6. The continuous black line is the digitized data in figure 5.a in that reference, and the dot-dashed curve corresponds to the Fraunhofer pattern reconstructed from the data reported in figure 5.b.

In general, we find that the data for the HgCdTe-HgTe system of Ref. 20 shows more consistency with the Dynes-Fulton analysis than the data of Ref. 21 on the InAs-GaSb system. For example, the extracted current distribution in Ref. 21 consistently spreads out way outside the nominal sample boundary which is unphysical, and may be pointing toward the inapplicability of one of the assumptions about the underlying physics.

[1] X.-L. Qi and S.-C. Zhang, Rev. Mod. Phys. **83**, 1057 (2011).
[2] A. Y. Kitaev, Physics-Uspekhi **44**, 131 (2001), cond-mat/0010440.
[3] G. Volovik, JETP Lett. **70**, 609 (1999).
[4] N. Read and D. Green, Phys. Rev. B **61**, 10267 (2000).
[5] C. Nayak, S. H. Simon, A. Stern, M. Freedman, and S. Das Sarma, Rev. Mod. Phys. **80**, 1083 (2008).
[6] F. Wilczek, Nature Physics **5**, 614 (2009).
[7] D. A. Ivanov, Phys. Rev. Lett. **86**, 268 (2001).
[8] L. Fu and C. L. Kane, Phys. Rev. Lett. **100**, 096407 (2008).
[9] L. Fu and C. L. Kane, Phys. Rev. B **79**, 161408 (2009).
[10] J. D. Sau, R. M. Lutchyn, S. Tewari, and S. Das Sarma, Phys. Rev. Lett. **104**, 040502 (2010).
[11] R. M. Lutchyn, J. D. Sau, and S. Das Sarma, Phys. Rev. Lett. **105**, 077001 (2010), arXiv:1002.4033.
[12] Y. Oreg, G. Refael, and F. von Oppen, Phys. Rev. Lett. **105**, 177002 (2010).
[13] J. D. Sau, S. Tewari, R. M. Lutchyn, T. D. Stanescu, and S. Das Sarma, Phys. Rev. B **82**, 214509 (2010).

[14] V. Mourik, K. Zuo, S. M. Frolov, S. Plissard, E. A. Bakkers, and L. Kouwenhoven, Science **336**, 1003 (2012).

[15] A. Das, Y. Ronen, Y. Most, Y. Oreg, M. Heiblum, and H. Shtrikman, Nature Physics **8**, 887 (2012), arXiv:1205.7073.

[16] M. T. Deng, C. L. Yu, G. Y. Huang, M. Larsson, P. Caroff, and H. Q. Xu, Nano Letters **12**, 6414 (2012), arXiv:1204.4130.

[17] A. D. K. Finck, D. J. V. Harlingen, P. K. Mohseni, K. Jung, and X. Li, Phys. Rev. Lett. **110**, 126406 (2013).

[18] H. O. H. Churchill, V. Fatemi, K. Grove-Rasmussen, M. T. Deng, P. Caroff, H. Q. Xu, and C. M. Marcus, Phys. Rev. B **87**, 241401 (2013).

[19] L. P. Rokhinson, X. Liu, and J. K. Furdyna, Nature Physics **8**, 795 (2012).

[20] S. Hart, H. Ren, T. Wagner, P. Leubner, M. Mühlbauer, C. Brüne, H. Buhmann, L. W. Molenkamp, and A. Yacoby, Nature Physics **10**, 638 (2014).

[21] V. S. Pribiag, A. J. A. Beukman, F. Qu, M. C. Cassidy, C. Charpentier, W. Wegscheider, and L. P. Kouwenhoven, ArXiv e-prints (2014), 1408.1701.

[22] M. Konig *et. al.*, Science **318**, 766 (2007).

[23] I. Knez, R.-R. Du, and G. Sullivan, Phys. Rev. Lett. **107**, 136603 (2011).

[24] K. C. Nowack, E. M. Spanton, M. Baenninger, M. König, J. R. Kirtley, B. Kalisky, C. Ames, P. Leubner, C. Brüne, H. Buhmann, et al., Nat. Mater. **12** (2013).

[25] E. M. Spanton, K. C. Nowack, L. Du, G. Sullivan, R. R. Du, and K. A. Moler, Phys. Rev. Lett. **113** (2014).

[26] I. Knez, R.-R. Du, and G. Sullivan, Phys. Rev. Lett. **109**, 186603 (2012).

[27] R. C. Dynes and T. A. Fulton, Phys. Rev. B **3**, 3015 (1971).

[28] M. Tinkham, *Introduction to Superconductivity* (McGraw-Hill, 1996), 2nd ed.

[29] K. K. Likharev, Rev. Mod. Phys. **51**, 101 (1979).

[30] H. H. Zappe, Phys. Rev. B **11**, 2535 (1975).

[31] W. Haberkorn, H. Knauer, , and J. Richter, Phys. Status Solidi A **47**, K161 (1978).

[32] A. A. Golubov, M. Y. Kupriyanov, and E. Il'ichev, Rev. Mod. Phys. **76**, 411 (2004).

[33] I. O. Kulik and A. N. Omelyanchuk, Fiz. Nizk. Temp. **3**, 945 (1977).

[34] S.-P. Lee, K. Michaeli, J. Alicea, and A. Yacoby, ArXiv e-prints (2014), 1403.2747.

[35] G. Tkachov, P. Burset, B. Trauzettel, and E. M. Hankiewicz, ArXiv e-prints (2014), 1409.7301.

[36] C. Ishii, Prog. Theor. Phys. **44**, 1525 (1970).

[37] A. V. Svidzinsky, T. N. Antsygina, and E. N. Bratus, J. Low Temp. Phys. **10**, 131 (1973).

[38] B. Zhou, H.-Z. Lu, R.-L. Chu, S.-Q. Shen, and Q. Niu, Phys. Rev. Lett. **101**, 246807 (2008).

[39] H.-Y. Hui, J. D. Sau, and S. Das Sarma, ArXiv e-prints (2014), 1401.3010.

[40] H. Choi, I. Sivan, A. Rosenblatt, M. Heiblum, V. Umansky, and D. Mahalu, ArXiv e-prints (2014), 1409.4427.